Examination of the DL Based Ubiquitous MIMO U/L NOMA System Considering Robust Fading Channel Conditions for Military Communication Scenario

RAVI SHANKAR, MANOJ KUMAR BEURIA,
GOPAL RAMCHANDRA KULKARNI, ABU SARWAR
ZAMANI, PATTETI KRISHNA AND V. GOKULA KRISHNAN
Electronics and Communication Engineering Department
Madanapalle Institute of Technology and Science
Madanapalle, 517325 India
E-mail: ravishankar@mits.ac.in; {drgopalrkulkarni; kpatteti}@gmail.com; a.zamani@psau.edu.sa

In this work, we investigate the end-to-end performance of the uplink (U/L) non-orthogonal multiple access (NOMA) system based on the novel Bi-directional long short-term memory (Bi-LSTM) algorithm over the frequency flat independent and identically distributed (i.i.d.) Rayleigh fading channel conditions. When compared to conventional successive interference cancellation (SIC) MIMO-NOMA-based detection systems, the suggested deep learning (DL) based technique integrates the conventional multiple-input multiple-output (MIMO) and power-domain NOMA schemes to improve the symbol error rate (SER) performance. To this end, an optimal power allocation problem for the MIMO-NOMA scheme has been developed that maximizes the data throughput of the end-to-end system. In this work, both imperfect and perfect SIC schemes are considered, and performance comparison is provided between the Bi-LSTM based MIMO-NOMA and LSTM MIMONOMA schemes. The SIC NOMA system achieves 15 dB for 10^6 iterations, but the DL-based MIMO-NOMA scheme achieves 15 dB for 100 iterations. By a factor of four, Bi-LSTM MIMO-NOMA schemes outperform SIC MIMO-NOMA methods. Rather than utilizing conventional SIC systems to determine fading channel coefficients and decode signals, the suggested scheme estimates the relevant data symbol using the more efficient Bi-LSTM algorithm. There is a 4 dB difference, indicating that DL-based MIMO-NOMA outperforms conventional SIC MIMO-NOMA approaches. Furthermore, when the channel estimation error is enhanced from 0 to 1, the performance of DL is considerably decreased. Even with perfect channel state information (CSI), the DL detector outperforms the SIC detector for channel estimate errors of less than 0.07. When differences between the real and predictable channel states occur, the DL detector's performance suffers significantly, yet it can still maintain its majority within a predetermined tolerance range

Keywords: signal-to-interference-and-noise ratio (SINR), long short-term memory, millimeter-wave (mmWave), signal-to-noise ratio (SNR), NOMA, DL, machine learning (ML)

1. INTRODUCTION

Fifth-generation (5G) wireless technology is significant not just because it can handle millions of user devices at ultra-high speeds, but because it also has the potential to change people's lives all around the world. However, as the number and variety of devices

increase, the same radio frequency (RF) spectrum must be used repeatedly for multiple applications and/or users. Moreover, the Internet of Things (IoT) requires everyone and every device to be connected [1, 2]. The rapid development of wireless communication standards has enabled individuals with faster and more dependable access to information anytime and everywhere, and the advent of digital wireless communication has made our lives simpler and more appropriate than ever before [3]. Thanks to several unique data transmission technologies, today's 5G wireless networks can deliver peak data speeds of 30 gigabits per second (Gbps) and average data rates of 200 megabits per second (Mbps) [4]. The research community and industry have presented some feasible 5G wireless schemes to meet the stringent standards and handle future generations' issues [5]. For example, the vehicular-to-infrastructure (V2I) communication scheme is proposed to increase the channel capacity and end-to-end reliability for very high-speed vehicular communication systems in time-selective fading channel scenarios. The massive-MIMO scheme is presented to improve transmission bandwidth, spectral efficiency (SE), and energy efficiency (EE). The mmWave technology is proposed to get higher data transfer rates, high reliability, and higher security [6, 7]. Using a high number of small-sized cells, ultra-dense networks are investigated to increase network throughput and minimize energy usage. In addition to the techniques, researchers are working on a new radio access scheme that will be utilized in 5G wireless networks since it can increase data rate and transmission bandwidth [8, 9].

Researchers have recently focused their attention on non-orthogonality-based system designs for usage in 5G networks [10, 11]. Multiple access (MA) schemes are broadly classified into orthogonal and non-orthogonal-based transmission schemes. To mitigate the effect of the multiple user interference (MUI), the orthogonal carrier-based transmission, such as the orthogonal multiple access (OMA) scheme enables each user's equipment to use orthogonal communication resources within a specific time slot, frequency range, or code. In 5G-NOMA the multiple users can use non-orthogonal resources, resulting in a significant increase in SE while permitting some degree of receiver interference for MA. NOMA has attracted the interest of numerous academics to enhance SE and EE and satisfy the demands of wireless users for end-to-end reliability, congestion-free networks, and massive connectivity [12]. The basic idea of 5G-NOMA is that several wireless users may be served by sharing the same physical resource at varying power levels. Specifically, the superposition coding method is used at the base station (BS), while the SIC scheme is used at the receiver to decode the signals of many users [13]. More power is allocated to wireless users with poor channel gains, where NOMA may deliver services to many users, to preserve user fairness. Even though OMA strategies may achieve high EE and SE even with basic receivers in an ideal scenario due to minimum MUI among wireless users, they are still unable to resolve the rising issues posed by increasing demands in 5G and beyond 5G (B-5G) networks, for example, should cover three primary kinds of scenarios, including improved voice, video, and data, according to the 3rd generation partnership project (3GPP) for 2020 and beyond [15]. Extreme mobile broadband (eMBB), ultra-reliable low-latency communication (URLLC), and massive machine type communication (MTC) are three possibilities that 5G technology is expected to enable. The key challenges in the eMBB scenario are a user-perceived transmission rate of 200 Mbps and a more than three-fold increase in SE over prior long-term evolution (LTE) advanced releases to enable services such as augmented reality (AR),

high transmission bandwidth, virtual reality (VR), higher throughput, and high-definition (HD) video experience [15, 16]. Various technologies related to the 5G-IoT network are schematically depicted in Fig. 1 [17]. Since many IoT devices would have access to the 5G wireless network, MTC's main challenge will be to achieve a connection density of 5 million devices per square kilometer. The major criteria for URLLC are 0.4 milliseconds end-to-end latency and 99.999 % end-to-end reliability. For VR and AR applications, the NOMA technique might potentially raise the number of IoT devices by 5 and 9 times, respectively [13–15]. Furthermore, in eMBB, NOMA was shown to be 35 % more spectrum efficient for downlinks (D/Ls) and 100 % more spectral efficient for U/Ls when compared to OMA [16]. Consequently, NOMA has been chosen as a strong candidate among all MA approaches because it possesses key qualities that enable it to overcome OMA challenges while also satisfying the needs of 5G and B-5G systems. The variables are summarized in Table 1 for better understanding and clarity.

Table 1. Variables.

Notation	Variable Type	Notation	Variable Type
X	Composite Signal at the BS	$|g_l|^2$	l^{th} user channel gain
β_l	Power allocation factor of the lth user	K_l	$l^{tb}\,user's$ symbol vector length
P_x	Total power transmitted from the Base Station	N_l	Additive white Gaussian noise (AWGN) sample
s_l	Signal transmitted from the lth user	Φ^2	Noise Variance
L	Total number of antennas user	Z_l	Small scale fading channel matrix
N	Total number of user equipment	T_1^U	1st users transmit symbol vectors
P_1^U	$l^{tb}\,user's$ transmit power	T_2^U	2nd users transmit symbol vectors
η'^U	AWGN vector	$E\left(.\right)$	Expectation operator

1.1 Basic Concepts of NOMA

This research utilizes SINR and throughput analysis to provide an overview of the D/L NOMA network. Following that, a high SNR study was carried out to compare the performance of the OMA and NOMA approaches. As seen in Fig. 2 [14], the BS sends the superimposed signal to the various user equipment based on their power allocation factor values at the transmitter (Tx) side of the D/L NOMA network. The SIC process should be run consecutively at each user's receiver until the user's signal is recovered. The optimal power allocation factors are assigned in an inversely proportional manner based on their fading channel scenarios. A wireless user with a low channel gain receives more power than a user with a strong fading channel gain. Therefore, the user with the bad channel condition recovers its signal without using the SIC approach, since the other users' signals are considered noise. Other users, on the other hand, insist on performing SIC schemes. The SIC system detects signals that are larger than the user's intended signal first. After subtracting the signals from the receiving signal, the procedure is repeated until the linked user's signal is retrieved. Finally, by neglecting users with lower power allocation factors, each user decodes their signal. The following is a representation of the sent signal at the

BS [14–17],

$$X = \sum_{l=1}^{N} \sqrt{\beta_l \mathrm{P}_x s_l}, \tag{1}$$

where s_l is the lth user equipment (UE_l) information with $E\left(|s_l|^2\right) = 1$, *i.e.*, unit energy symbol. The total power transmitted from the BS is represented as P_x and β_l represents the lth user power allocation factors subject to: $\sum_{l=1}^{N} \beta_l = 1$, and $\beta_1 \geq \beta_2 \geq \cdots \geq \beta_N$. Since the users with weak channel strength have a high power allocation factor as compared to strong channel gain users, the channel gains are arranged as follows: $|g_1|^2 \leq |g_2|^2 \leq \cdots \leq |g_N|^2$, where l^{th} user channel coefficient is represented as g_l based on the power domain NOMA concept. The signal received by the lth user can be written as follows [14–17]:

$$y_l = g_l X + \mathrm{N}_l = g_l \sum_{l=1}^{N} \sqrt{\beta_l \mathrm{P}_x s_l} + \mathrm{N}_l, \tag{2}$$

where N_l is AWGN noise sample having zero average value and variance of Φ^2, *i.e.*, $N_l \sim \left(0, \Phi^2\right)$.

1.2 Literature Survey

DL is an ML method that allows computers to learn by example in the same way that people do. The system understands the useful items within, learns characteristics and patterns, and solves issues by interpreting the incoming data on feeding. In the review work [18], the authors give a detailed investigation of DL-assisted communication. The history and significance of DL are examined. The authors discuss the relevance of DL in prospective wireless methods such as MIMO, NOMA, and mmWave. In a NOMA-assisted wireless communication system, a schematic of the DL scope is shown in Fig. 3 [18]. The authors discuss the problems, possibilities, and future research directions for DL in the wireless environment. In a DL-aided NOMA system, it has been demonstrated how to enhance SE, EE, data rate, and CSI. The direction of arrival and estimations of large-scale MIMO channels are studied using a DL-aided MIMO system. In mmWave communication, DL performance is investigated with extremely high-power consumption and limited link gains. In the work [17], the authors examine 2 single-cell to k-user multi-cell wireless networks utilizing OMA schemes to offer a comprehensive assessment of D/L NOMA. Different NOMA system elements and problems, such as SIC, power allocation factor, CSI, and inter-channel interference (ICI), are comprehensively examined. Furthermore, the impact of ML and DL on the 5G-NOMA system is investigated. In [18], the authors examine the advantages of DL-assisted NOMA channel estimation and detection. The authors present a comprehensive examination of 5G-NOMA system problems and examine the possibility of DL. The examination is divided into three sections: optimal power allocation, channel decoding, and 5G waveform design. The opportunity and shortcomings of DL-assisted NOMA in 5G networks are examined in this review paper. Offline and online training are two forms of training identified in the MIMO-NOMA network. Fig. 4 demonstrates the DL-based NOMA model [20]. The hidden layer is utilized for classification and training. Multiple neurons are found in large quantities in hidden layers. A layer in Fig. 4 is the noise layer, which can be used to contaminate the processed signal using AWGN. With the help of current fading channel models and extensive input data formation, CSI knowledge can be acquired automatically. Offline training involves
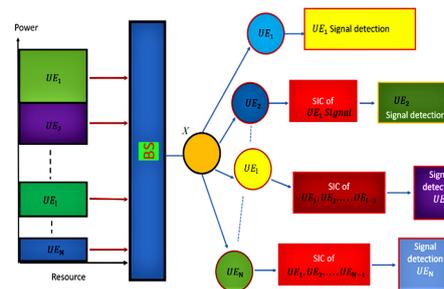
Fig. 1. Technologies associated with 5G-IoT.

Fig. 2. D/L NOMA network.

appropriately training arbitrary sequences of input symbols using CSI information learned from simulations for real-time propagation circumstances. With the training data, the output signals may be utilized to precisely predict the fading channel coefficients. The pilot symbols are used for gaining knowledge of the CSI in the online training phase, and after the training of the input signals is done using this information. A block schematic of the NOMA system for CSI auto-detection with online and offline training is shown in Fig. 5. In the case of adverse wireless conditions such as bad weather or heavy rain, the DL scheme can also be employed to detect the fading channel. The LSTM strategy is employed to detect the fading channel coefficients in the event of time-selective fading channel scenarios, such as in the vehicular-to-vehicular (V2V) wireless network. Hidden layers can act as a network state memory, in this case, allowing the DL to save, remember, and explore the complex data symbols that came before it.

The optimal resource allocation is a significant factor in determining the outage and end-to-end system performance of the NOMA system. In the case of multiple users, the DL algorithm is a potential strategy for solving the problem of optimal power allocation. Furthermore, dynamic power allocation is challenging under time-selective fading channel circumstances. Maximizing energy utilization through efficient resource allocation is an important research problem using NOMA. Several ML algorithms have been developed to handle this problem. In the work [21], the authors have proposed a deep belief network (DBN) as a DL technique for maximizing the total available power at the BS. The problem of dynamic power allocation may also be addressed with deep reinforcement learning (DRL). DRL develops an optimal power allocation framework using a deep deterministic policy gradient (DDPG), and Q-learning is utilized to investigate the resource allocation problem. The classic SIC model has several flaws. When cellular traffic grows, using the SIC technique to correctly encrypt data becomes increasingly difficult. Propagation error has an impact on the SIC system as well. Signal classification allows the deep neural network (DNN) to recover a discrete data sequence from a decaying signal [22]. Using DL, the SIC system might be much improved. The authors have proposed an online learning detection strategy for NOMA U/L transmission in their work [23] to improve the SE. Another use of DL in NOMA might be in constellation design. As the data is delivered, the constellations of several users are superimposed. The basic idea is that the input source bits are translated into symbol sequences using DL after being modulated. To improve EE, an extra layer called the normalizing layer is constructed to link the
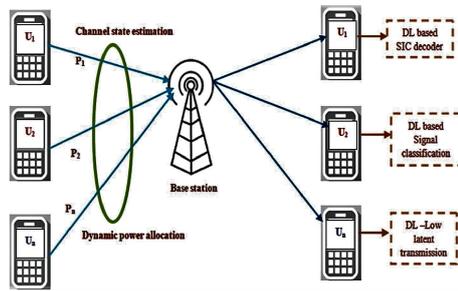
Fig. 3. A diagram of the DL scope in a NOMA-assisted wireless communication system.
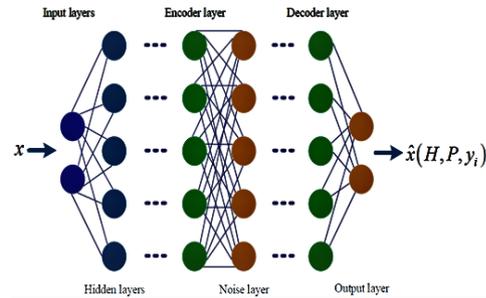

Fig. 4. Schematic representation of the DL-based NOMA model.

transmitter. In the work [24], the authors investigate an autoencoder-based DL strategy for optimizing constellation design. The technique developed is beneficial for multi-user access in a variety of channel situations. In NOMA, DL may also be utilized for latency optimization, subchannel matching and, power reduction. In the work [19, 25, 26], recent research efforts in 5G-IoT networks are thoroughly examined and the authors investigate the shortcomings that massively networked devices provide in terms of channel assignment, user clustering, resource allocation, interference control, and network coverage extension. Furthermore, the concepts of DL schemes are examined, as well as the scope of the DL algorithm in resource management for IoT-assisted systems. Different types of DNNs are investigated in detail, as well as their recent contributions to wireless communication issues. The study advances research and knowledge of 5G and B-5G technologies such as AR, VR, NOMA, 5G heterogeneous networks, and machine-to-machine (M2M) communication. In the work [19], the authors investigate the optimal power allocation problem for home-based vehicular wireless communication. The DDPG approach is utilized in the proposed wireless network, and V2V communication functions as an agent that interacts with the unknown environment to acquire experience, with NOMA being used to allocate radio resources. Due to node mobility, the fading channel is no longer frequency flat, and it becomes time selective in nature. Due to time selectivity, channel coefficients change rapidly, and it is very difficult to estimate the coefficients correctly, especially for the V2V systems. In the proposed decentralized discrete-time and finite-state Markov decision processes, the DDPG approach is employed to tackle the resource allocation problem. After 125 epochs, the proposed DDPG approach outperforms the DQN-based algorithm by 26 % and achieves faster convergence than DQN. The proposed approach surpasses the random resource allocation scheme by more than 90Mbps for 50 automobiles and by 40Mbps over the DRL algorithm in terms of attainable data transmission rate. With 120 deployed vehicles and a payload of 1 Mb, the proposed DDPG achieves a 95 percent average delivery probability. Furthermore, with 60 deployed vehicles, it obtains a 95.6 percent delivery probability for a 1.6 Mb payload, whereas the DRL achieves an 80 % delivery probability for the same payload. Research gap: While the suggested technique solves the resource allocation problem, the proposed DDPG algorithm's convergence behavior must be explored to determine the ideal conditions.

In the work [25], the authors developed an approach to allocating energy-saving re-

sources for heterogeneous IoT 5G-NOMA networks. In cognitive relaying systems with IUI reduction, the proposed approach solves (a) imperfect SIC, (b) stepwise resource allocation for cellular and 5G-IoT wireless users, and (c) recurrent neural networks (RNN) is utilized to identify users based on rate demands in limited spectrum heterogeneous networks. In the orthogonal frequency division multiple access (OFDMA) system, no cellular user may access the channel, but in the low SINR regime, NOMA enables 25 % of cellular users to access the channel and shares the spectrum with IoT. The access ratio is unaffected by the target SINR. At 5 dB IoT target-SINR, NOMA achieves a greater sum rate at 2 bits per second than OFDMA. Research gap: The EE of 5G NOMA heterogeneous networks is decreased when the spectrum is shared among mobile users and 5G-IoT devices. In the work [26], the authors have investigated the DL-assisted cross-layer optimization NOMA network. The authors employ the NOMA in conjunction with the OFDMA scheme for video transmission. The users are categorized and seen as a multi-label classification problem. The DL-assisted cross-layer optimization NOMA network's highly complicated transmission blocks are changed with appropriate supervised learning DNN structures. All the layers in the research, except for the output layer, use the rectified linear unit (ReLU) activation function. The sigmoid activation function is used in the output layer. After the output layer, a post-processing technique is provided to improve user grouping. When both the application and physical layers are considered, the average SNR enhances to 40.37 with a variation of 0.0036 (video quality). The typical resource allocation of the NOMA system gives identical performance characteristics with and without DL, according to the research study. As a result, DL's importance must be examined. In the work [27], the authors examine the optimal power problem in a grant-free NOMA network. The advantage of the Grant-free NOMA is that it provides massive connectivity, allowing 5G-IoT devices to be connected in the 5G and B-5G wireless networks. The grant-free NOMA system's performance is further improved by DL enhanced user recognition and decoding. An auto-encoder is used as an alternative to a SIC detector, with the encoder to the user and the decoder to the receiver.

A multi-layer DL architecture is being developed for a grant-free NOMA for effective energy communications. The suggested DL-based detector improves the SNR by 16 dB over the usual SIC receiver for a Bose–Chaudhuri–Hocquenghem (BCH) code, resulting in a block error rate of 10^{-6} and a rate of 0.6. Research Gap: Because coding techniques are employed to increase the BER performance, the system's SE is the worst. In the NOMA-assisted system, resource management is a critical process. The computational complexity of typical resource management techniques is significant. In the work [28], the authors have proposed the efficient resource management problem by doing basic changes in DNN designs. The proposed algorithm considers the incorrect SIC at the detector, including user ordering and optimal power allocation based on a dynamically fluctuating channel. In optimal power allocation, the interior point method (IPM) is employed, allowing for a higher data transmission rate. Power levels are labeled in the fully linked DNN model. The user scheduling technique is then used to raise the throughput even higher. DNN obtains a 90.67 % sum rate using a 22-bit input. The proposed power distribution system provides a total throughput of 15 bits/sec/Hz, which is 3 bits/sec/Hz faster than the single IPM method. Research gap: Unsupervised learning can be considered as part of the resource allocation approach to the practical system. In their research [28], the authors used the NOMA system for massive connectivity in a wireless IoT network.

The IoT network relays data from IoT devices to faraway servers using solar-powered unmanned aerial vehicles (UAVs). The UAV uses the conventional SIC channel estimator and detector to decode data from many devices, whereas IoT devices employ the slotted aloha medium access protocol. To achieve better throughput, a DRL-based optimization method was designed to handle the problem of dynamic channel access probability. In comparison to a system without DRL, the suggested method yields an 83 % better temporal average channel capacity. Research gap: DRL-based resource management might be built since the suggested model comprises huge IoT devices. The authors of [29] discuss resource allocation difficulties in NOMA-assisted cache-based mobile edge computing. To allocate resources, an LSTM algorithm-based network is utilized to process requests for computational task requests. To examine the long-term resource allocation strategy, a single-agent Q-learning algorithm has been designed. In addition, Bayesian learning-assisted multiagent Q-learning is used to offload choices to choose optimum actions at each state. By expending 60-time slots, the suggested approach predicts real job popularity with a probability of 0.10. Research gap: The proposed scheme is designed for a larger number of requests for computing tasks. According to the study work described above, different DL frameworks are employed in different types of NOMA-aided systems to optimize the resource allocation problem via DL. The DDGP algorithm was used in the V2V [19] communication search to dramatically improve BER performance and outage probability. Similarly, [28] indicates a significant increase in attaining channel capacity using the DRL technique. BiLSTM-based modeling outperforms traditional LSTM-based models in terms of prediction. BiLSTM models outperform autoregressive integrated moving average and LSTM models in terms of prediction. In their study [30], the authors employed a Bi-LSTM based DL technique to estimate fading channel coefficients in a variety of multipath circumstances. The performance of the Bi-LSTM algorithm is evaluated about the number of pilot symbols and cyclic prefixes. The BER statistics show that the Bi-LSTM scheme outperforms state-of-the-art channel estimation approaches such as the minimal mean square and error (MMSE) estimation method. The main contribution of the paper is given below: (i) Due to the advantage of the Bi-LSTM over the LSTM algorithm, the Bi-LSTM algorithm is used for the U/L NOMA wireless network instead of the traditional SIC NOMA receiver. (ii) We employ the Bi-LSTM algorithm to solve imperfect SIC problems that are not processed by conventional NOMA receivers. The proposed Bi-LSTM technique would decrease the gaps caused by imperfect SIC while also increasing the net throughput of the decoded signal. (iii) The simulation results demonstrate how numerous DL system parameters are considered. There are several elements to consider, including the number of users, epochs, suitable power allocation parameters, batch size, modulation types, and learning rate. According to the simulation findings, the proposed system outperforms the classic SIC technique.

2.   MIMO-NOMA DL SYSTEM MODEL

2.1   Channel Model

We examine a 5G-NOMA system that contains a BS with L antennas and two users, each user equipment is equipped with $G_l, l = 1, 2$, antennas. For the sake of simplic-

ity, the number of paired users for both U/L and D/L is limited to two. Expanding the suggested MIMO-NOMA techniques to more than two users while keeping their desired characteristics of IUI-free communication appears to be a difficult task that is outside the scope of this research. Furthermore, we assume that the user closest to BS is the second, and the user farthest away from BS is the first, resulting in a higher path loss. It is critical to pair users who are experiencing distinct channel conditions to reap the benefits of NOMA [31, 32]. Between the l^{tb} user, $l = 1, 2$, and the BS, the D/L MIMO channel is described as [31–34],

$$\frac{1}{\sqrt{\Pi_l}} Z_l, \tag{3}$$

Small scale fading or fast fading effects are represented by the elements of the matrix $Z_l \in {}^{G_l \times L}, l = 1, 2$. Furthermore, $Z_l \in {}^{G_l \times L}, l = 1, 2$. denotes the route loss between the BS and the l^{tb} user [31][26], which models the uplink MIMO channel between the l^{tb} user and the BS as shown below [31].

$$\frac{1}{\sqrt{\Pi_l}} Z_l^{\mathrm{H}}, \tag{4}$$

Additionally, it has been assumed that both MIMO matrices Z_1 and Z_1 have perfect knowledge of the CSI [31, 32].

2.2   U/L NOMA Data Transmission Model

Let $K_l = \min\{G_l, L\}; l = 1, 2$ be the $l^{tb} user's$ symbol vector length, and $T_1^U = [T_{1,1}^U, \ldots, T_{1,K_1}^U]^T \in {}^{K_1 \times 1}$ and $T_2^U = [T_{2,1}^U, \ldots, T_{2,K_2}^U]^T \in {}^{K_2 \times 1}$ represent the 1st 1st and 2nd 2nd users transmit symbol vectors, respectively. In this investigation, we have considered that $T_{l,m}^U \sim (0, 1)$, $l = 1, 2$, $m = 1, 2, \ldots, K_l$, are frequency-flat i.i.d. Rayleigh fading links in this example. For the sake of evaluating the attainable user rates for MIMO-NOMA [31–34], we assume perfect Gaussian signaling. Using a linear precoder matrix $P_l^U \in {}^{G_l K_l}, l = 1, 2$, the l^{tb} user precodes and sends a symbol vector. There are known modulation and coding methods that may nearly match the performance of perfect Gaussian signaling and can be employed in practical implementations, such as [34], where the l^{tb} user precodes them transmit symbol vector using a linear precoder matrix P_l^U. To communicate their precoded symbol vectors to the BS, both users use the same resource. The $l^{tb} user's$ transmit power $P_l^U, l = 1, 2$ is expressed as [31],

$$P_l^U = tr\left(P_l^U \left(P_l^U\right)^H\right). \tag{5}$$

The received signal at the BS, $y'^U \in {}^{L \times 1}$, is given by [30–33],

$$y'^U = \frac{1}{\sqrt{\Pi_1}} H_1^H P_1^U T_1^U + \frac{1}{\sqrt{\Pi_2}} H_2^H P_2^U T_2^U + \eta'^U. \tag{6}$$

At the BS, the letter $\eta'^U \sim \left(0, \sigma^2 I_L\right)$ stands for the AWGN vector. The received signal at the BS is first processed using a unitary detection matrix $Q^U \in {}^{L \times L}$ to generate [25, 31],

$$y = Q^U y'^U = \frac{1}{\sqrt{\Pi_1}} Q^U H_1^H P_1^U T_1^U + \frac{1}{\sqrt{\Pi_2}} Q^U H_2^H P_2^U T_2^U + \eta^U, \tag{7}$$

which is then decoded. Where $\eta^U = Q^U \eta'^U \sim \left(0, \sigma^2 I_L\right)$ is subsequently used for decoding.

2.3   DL Based NOMA System

DNN, convolutional neural network (CNN), and RNN are among the most common DL strategies. The fundamentals of various DL-based schemes are briefly discussed in this section. The DNN is a more advanced form of the neural network, with three layers:

output, input, and hidden. The hidden layers may be extended to many layers according to the complexity of the signal processing method. The effects are only applied to nearby levels, and each layer comprises many nodes. Fig. 4 gives the schematic representation of a DNN model. Linear and nonlinear relationships exist between neighboring layers. Each layer's linear relationship between input and output is controlled by the linear component. The two types of operations are multiplication (denoted by the weight $\tilde{m}$) and addition (denoted by the bias $\tilde{t}$). However, in most real-time propagation scenarios, we are confronted with nonlinear issues that cannot be handled using the linear technique. As a consequence, the nonlinear component is handled using the activation function, the nonlinear component is handled using the activation function $f(.)$. Assume that the $(l-1)^{th}$ layer's output is y_{l-1}, the lth layer's weight matrix is $\tilde{m}_l$, the bias vector is $\tilde{t}_l$, and the lth layer's output y_l may be denoted as follows:

$$y_l = f(\tilde{m}_l.y_{l-1} + \tilde{t}_l), \tag{8}$$

The sigmoid function is a classic activation function for DNNs (9). The function's range is restricted to [0, 1], and it can only approximate the probability. The tanh function (10) is a standard activation function as well. The range of the tanh function is expanded to [-1, 1], and the output center of each layer is adjusted to 0, resulting in faster convergence using stochastic gradient descent (SGD). Another important activation approach is the rectified linear unit (ReLU) function (11). The ReLU function rises linearly when $u > 0$ and is zero when $u < 0$, rather than confining the value to [0, 1] or [–1, 1]. After repeated nonlinear procedures, the gradient does not vanish.

$$f_{sig}(u) = \frac{1}{1+\exp(-u)}, \tag{9}$$

$$\tanh(u) = \frac{e^u - e^{-u}}{e^u + e^{-u}}, \tag{10}$$

$$\text{Re}LU(u) = \begin{cases} u & ,u \geq 0 \\ 0 & ,u < 0 \end{cases} \tag{11}$$

The transmission equation for several hidden layers may be defined as follows, assuming that the bias is 0 for simplicity.

$$y_n = f(\tilde{m}_n f(\tilde{m}_{n-1} f \ldots \tilde{m}_2 f(\tilde{m}_1 y_0)) \tag{12}$$

The sigmoid function (9) and the softmax function are the most frequent choices for the output layer. The softmax function, which is mostly used for multiclass classification, is defined as follows:

$$f_{soft}(u)_i = \frac{e^{u_i}}{\sum_j e^{u_j}}. \tag{13}$$

In DL algorithms, we frequently need to input the system a large amount of data, known as the training set, so that it can modify itself adaptively to the optimal status offline. Correct data should be utilized during the training phase to correct the result. Then, a supervised relationship between the input and the output may be constructed. The trained system may then be applied to the test set to evaluate the DNN's performance. To increase and allow the full potential of 5G, DL schemes are being applied. DL schemes popularity began to rise in the early 2000s, but it was not until lately that DL became more widely used. DL can understand, produce, and investigate practically any task given to it, producing concise and trustworthy outcomes. It boasts cutting-edge performance,

and some of its notable achievements include VR, AR, image classification, and object identification. DL algorithms are developed in a variety of disciplines, including wireless networks and 5G, to provide more rapid, more consistent, and more trustworthy outcomes using simple techniques [34, 35]. In [35], the authors have uncovered new research results in the following five 5G schemes: low-density parity-check coding, efficient power allocation in NOMA networks, massive MIMO, and security. Millimeter-wave blockage prediction, resource allocation in code domains NOMA, SE, EE, and channel capacity are the major topics in 5G and B-5G communication. The 5G and B-5G schemes include optical free-space communication, reconfigurable intelligent surfaces, visible light communication, Terahertz communication, and UAVs that may employ DL. Data processing is growing increasingly difficult and diversified, as is obtaining the optimal CSI. By successfully training these complicated data symbols, better performance may be produced. DRL is a kind of DL technique that is considered crucial in 5G MIMO-NOMA wireless communications [36]. The most well-known use of the DRL method thus far has been resource management. Prior knowledge of the CSI is not necessary for generating results in the Q-learning-based DRL scheme.

3.   RNN BASED DL ALGORITHM

A feed-forward neural network allows information to travel only in one direction: from the input nodes to the output nodes, passing via the hidden layers. In the network, there are no loops or cycles. Because they are meant to extract contextual information by specifying the connections between multiple time steps, RNN [7,8] is a type of NN that is commonly employed in the sequence analysis process. An RNN is made up of a series of recurrent layers that are modeled successively to map one sequence to another. RNN has a great capacity to extract contextual information from a sequence. Contextual signals in the network structure, on the other hand, are consistent and successful in data classification. RNN is capable of processing sequences of any length. The RNN classifier's architecture is depicted in Fig. 6. RNNs function by maintaining a layer's output and feeding it back into the input to anticipate the layer's output. RNNs, which are cutting-edge algorithms for sequential information sequences, are used by virtual digital assistants such as Alexa, Google Home, Apple's Siri and, Cortana. It is the first read-only memory (ROM) algorithm to identify its input, making it perfect for ML challenges requiring sequential data symbols. RNNs are the only neural networks with internal memory, making them a very efficient and dependable form of neural network. The existence of loops in hidden layers extends feedforward NN to RNN. An RNN takes a sequence of samples as input and calculates the temporal connection between them. In RNNs, it is easier to remember past data because of the presence of internal memory, resulting in accurate prediction. RNNs are therefore the most effective way to process audio, text, time series, and a variety of other forms of sequential data. Unlike other DL algorithms, RNNs have the potential to produce a far more thorough interpretation of a sequence's meaning. Due to its ability to memorize data, the RNN is another popular topic in natural language processing (NLP) research. By creating a link between the present and past data, RNNs can cope with situations where sequences from distinct slots have associations with each other (and even future data). Fig. 7 shows the fundamental structure of an RNN. The preceding data is
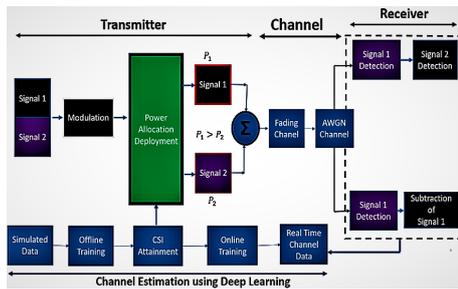
Fig. 5. NOMA system block diagram with online and offline CSI auto-detection training.
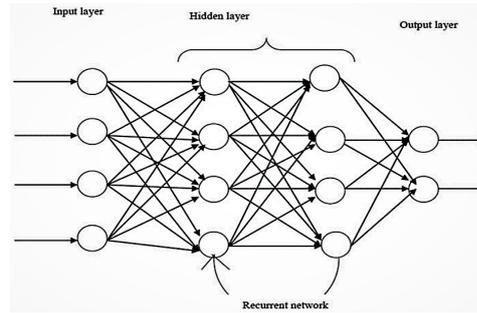

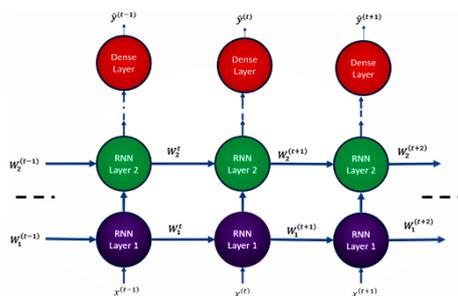Fig. 6. Schematic representation of the RNN classifier.

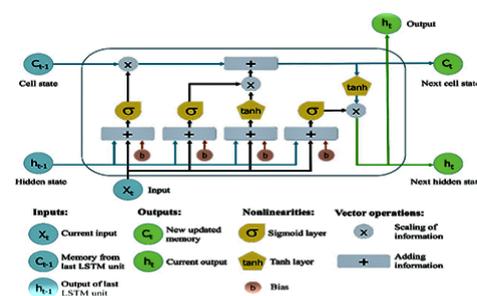Fig. 7. Block diagram representation of the RNN [33].

Fig. 8. Block Diagram representation of the LSTM algorithm [36-38].

summarized as a state $W_k^{(t)}$ for solving the output $\hat{y}^{(t)}$ with the present input. The number of RNNs outputs may differ from the number of inputs in a variety of applications, including 5G signal processing, sentiment analysis and classification, and machine translation.

3.1   LSTM Scheme

LSTM networks are an RNN enhancement that effectively increases memory. The LSTM handles classification issues by integrating network parameters with the hidden node and releasing the state based on input data. As a result, it is highly suited to learning from large events separated by extended periods. The layers of an RNN, also known as an LSTM network, are built with LSTM network units. RNNs may store inputs for a long period because of LSTMs. This is since LSTMs store data in a computer-like memory. Fig. 8 shows the LSTM algorithm. The LSTM is capable of erasing, writing, and reading data from its memory [37].

3.2   Proposed Bi-LSTM Scheme

Two separate hidden layers are used to process the network in two directions: backward and forward. In the work [21], the authors demonstrate that the Bi-LSTM networks outperformed unidirectional networks in scenarios like phonemic grouping, according to

the authors of [21]. Fig. 9 shows a schematic illustration of the RNN algorithms. The output of both the backward and forward layers is calculated in the same way as the unidirectional RNN. The output Y_t of the Bi-LSTM method is given as [22],

$$Y_t(\vec{h}_t, \overleftarrow{h}_t), \tag{14}$$

where $Y_t(\vec{h}_t, \overleftarrow{h}_t)$ signifies the backward layer result order and $\vec{h}_t$ denotes the forward output layer. Layers in all networks employ the dropout function, which is a mechanism for preventing network overfitting. This shows that learning occurs across several topologies and neuron types. Fig. 10 (a) shows the networks before and after dropout (b).

4. SIMULATION AND ANALYSES

In this sub-section, we investigate the end-to-end SER performance of the Bi-LSTM based MIMO-NOMA scheme and simulation outcomes have been demonstrated for various system parameters in Table 2. To begin, the SER performance of Bi-LSTM, LSTM, and SIC schemes has been examined for various modulation schemes under frequency flat i.i.d. Rayleigh fading channel circumstances. Second, in perfect and imperfect CSI circumstances, the SER performance of Bi-LSTM, LSTM, and SIC schemes is compared for various values of power allocation factors. We also ran simulations for various values of mini-batch sizes to speed up the convergence of the Bi-LSTM scheme. Finally, practical suggestions for accelerating training are given. For performing ML tasks, a variety of tools and software are available. We used Python 3.10.2 (open source), MATHEMATICA, the R programming language (open source), and MATLAB 2021b (licensed version) in the simulations because of their usability and computing efficiency. The suggested DL approach is built using graphics processing unit (GPU) acceleration, Azure ML Studio, and Google TensorFlow, which is a powerful open-source ML framework from Google. Given the imperfect CSI conditions, the fading channel is robust and frequency flat (i.i.d. Rayleigh fading). For simplicity, two-user U/L MIMO-NOMA has been used in the simulations, with each user equipment having six antennas. The MIMO fading channel model has a size of 6×6 with a single cluster that has been examined in this paper. In simulations, the total available power is limited to 1W, and the distant user or poor channel gain user receives almost all the available power for improved SER, while the user with good channel conditions receives less power (nearly 10 percent of total available power). Hidden layers have a sigmoid activation function [35], whereas output layers have a ReLU activation function [36]. The 500,900 number of data symbols and mini-batch (smaller data sets) are considered in this work for getting the faster convergence rate and optimal SER performance [20, 38].

In the supervised learning-based DL scheme, all the labels are one-hot encoded. The various simulation parameters are listed in Table 3. In the simulation, the DL MIMO-NOMA model is set up, and training data is generated and adjusted in a proper format. In the works [8–10], the authors have investigated the SER of the DL NOMA system considering the binary phase-shift keying (BPSK) and quadrature phase-shift keying (QPSK) symbols. In this work, we have considered the quadrature amplitude modulation (QAM) modulated data symbols in the SER analysis over Rayleigh distributed fading links. The simulations show that the SER performance increases considerably. The to-

Table 2. Variables.

Simulation Parameters	Assigned Values	Simulation Parameters	Assigned Values
Linux operating system	Windows 7 Enterprise	Tx Power = 1 W	Tx Power = 1 W
Simulation Software: Python 3.9.2 and MATLAB 2020b	Simulation Software: Python 3.9.2 and MAT-LAB 2020b	First UE power allocation factors = 0.80, second UE power allocation factor = 0.20	First UE power allocation factors = 0.80, second UE power allocation factor = 0.20
6×6 MIMO i.i.d. frequency flat fading links considering the AWGN noise	6×6 MIMO i.i.d. frequency flat fading links considering the AWGN noise	Hidden layer Activation function-Sigmoid Activation Function	Hidden layer Activation function-Sigmoid Activation Function
i.i.d. Frequency Flat Rayleigh Fading Links	i.i.d. Frequency Flat Rayleigh Fading Links	Output Layer Activation function-ReLU Activation Function	Output Layer Activation function-ReLU Activation Function
2 UEs per cluster	2 UEs per cluster	Number of Rx Antennas = 6	Number of Rx Antennas = 6
Number of Tx Antennas = 6	Number of Tx Antennas = 6	Training symbols=500,900	Training symbols=500,900
Google cloud auto machine learning tool box	Google cloud auto machine learning tool box		

tal number of slots is assumed to be M, and the input column vector is expressed as, $S = \left\{ S^{[1]}, S^{[2]}, \ldots, S^{[L]} \right\}$. At the lth time slot, the element of the column vector is $S^{[l]}$. The key system parameters, including as the output layer, output functions, learning rate, mini-batch, and hidden layer, have been set once the data has been generated and adjusted in the proper format. The DNN layer's bias and weight have now been initialized after this step. The forward DL technique is then used to achieve the required results, which is marked by $\hat{R}_l = \left\{ \hat{R}_l^{[1]}, \hat{R}_l^{[2]}, \ldots, \hat{R}_l^{[L]} \right\}$ [10]. The cross-entropy loss function for the average probability q is calculated as, $W(R, \hat{R}) = -R \times \log(q) - (1-r) * \log(1-q) ; R \in (0,1)$. The correction parameter values are computed and updated by utilizing the convex optimization and adaptive learning rate schemes. The data is tested once it has been trained, and then curves between the SNR in dB and the BER are shown.

There is a performance difference between DL-based MIMO-NOMA and standard SIC MIMO-NOMA systems. To access this gap, the suggested Bi-LSTM method is compared against the LSTM and SIC-based channel estimators. It has been assumed that the SIC scheme has correct information about the fading channel coefficients and that both user equipment and traditional SIC-based MIMO-NOMA detectors take into consideration QAM complex modulated signals. The 1st user signal is initially demodulated using
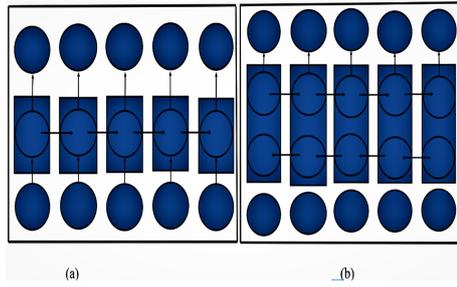
Fig. 9. The Schematic block diagram description of RNN DL models. (a) Unidirectional RNN, (b) Bi-directional RNN models [34].
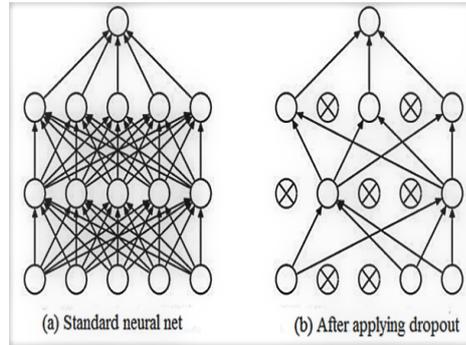

Fig. 10. Structure of networks (a) before and (b) after applying dropout [35].
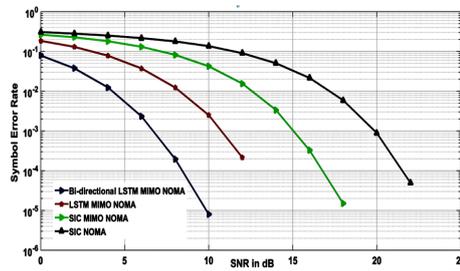

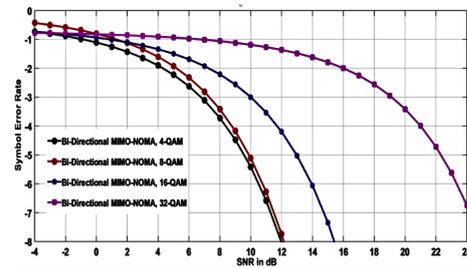Fig. 11. Performance comparison between the Bi-LSTM MIMO-NOMA, LSTM MIMO-NOMA, and SIC NOMA schemes.

Fig. 12. Bi-LSTM MIMO-NOMA-DL performance comparison for several modulation techniques.

the signal received from the second user as an interference signal in traditional SIC methods. The signal from the second user is recovered after subtracting the first user signal from the composite MIMO-NOMA signal obtained from the BS. However, in the Bi-LSTM MIMO-NOMA strategy, the received signal is forwarded to the DNN, and labels are established just for the second user sequence during the training phase. During the training phase, the input signal is introduced to the DNN detector input as a column vector, and only the second user data sequence labels are selected. As shown in Fig. 11, the conventional SIC NOMA system achieves 15 dB, whereas the Bi-LSTM MIMO-NOMA scheme achieves for iterations. The Bi-LSTM MIMO-NOMA schemes outperform the SIC MIMO-NOMA strategies by a factor of four. Instead of using conventional SIC schemes for determining the fading channel coefficients and decode signals, the proposed scheme uses the powerful Bi-LSTM algorithm to estimate the proper data symbol. In Fig. 12, simulations have been demonstrated for various modulation schemes. It is worth noting that no pre or post-processing is done. We have employed a sophisticated Bi-LSTM scheme to accomplish reliable signal recognition rather than typical complicated 5G signal processing for channel estimation and demodulation. User signals can utilize a variety of modulation schemes. Because in power domain NOMA, non-orthogonal carriers have been used, MUI particularly the type of modulation they use – has a huge impact

on demodulation performance. Table 3 shows three groups of stimulation parameter settings, including the scenarios where both user equipment had 4-QAM or quadrature QAM modulation and where (a) the First user used 4-QAM modulation, and second user used 4-QAM (first case) (b) First user used 8-QAM modulation, and second user used 8-QAM (second case) (c) the First user used 16-QAM modulation and second user used 16-QAM (third case) (d) First user used 32-QAM modulation and second user used 32-QAM (third case). Because the second user signal must be decoded first using the SIC approach, we only used the Bi-LSTM scheme to identify the second user signal owing to its higher signal processing complexity. Fig. 12 represents the SER performance in all four scenarios. The SER performance of the Bi-LSTM MIMO-NOMA system is demonstrated to be excellent. Aside from the previously mentioned example 1, case 1 resulted in a 4 dB performance rise, whereas case 4 resulted in a 1.5 dB gain. These results imply that the Bi-LSTM might be utilized to learn the Rayleigh distributed MIMO channel's fading channel coefficients, as well as signal demodulation using NOMA. In addition, optimal resource allocation is implemented, with various amounts of power allocated to different user equipment dependent on channel strength. Using QAM complex modulated signals, several user equipment are investigated in the simulation. Because the MIMO-NOMA scheme considers non-orthogonality, which is one of the most important determining factors in calculating SER performance, interference from other users must be addressed. The DL MIMO-NOMA detector outperforms SIC-based systems, as shown by the curves in Fig. 13. Aside from case 1, which had a 4 dB increase in output, scenario 2 saw a 1 dB improvement in performance. These outcomes show that the DL approach may be utilized to learn both the properties of the wireless MIMO Rayleigh fading channel and the symbol detection using NOMA. Fig. 14 represents the end-to-end performance of DL MIMO-NOMA systems employing 8-QAM complex modulated symbols and various power allocation channel coefficient values.The proposed method outperforms earlier approaches for all scenarios of power distribution channel coefficients. When the power allocation coefficient is equal to 0.90, the SER is the least, and the dynamic power allocation scheme outperforms the fixed power allocation approach significantly. The imperfect knowledge of the CSI has a significant impact on SER performance as well as the detection and estimation method during the training stage. The fading channel coefficients detection and estimation are done at the training phase. We investigated how the suggested Bi-LSTM scheme was accomplished when the estimated CSI differed from the real-time propagation scenario by presenting the error into the channel at the testing step. The relation between i.i.d. Rayleigh fading channel matric with channel error, represented as, Z and the actual channel matrix, represented as, $\hat{Z}$ is expressed as, $Z = \hat{Z} + \alpha\beta$. Where β represents the channel error matrix and α represents the error factor. During the testing phase, imperfect CSI is considered, and the effect of imperfect CSI on SER performance for the Bi-LSTM MIMO-NOMA scheme is shown in Fig. 15. The SER performance of the Bi-LSTM MIMO-LSTM system degrades dramatically as the value is increased from 0 to 1. Even when the perfect CSI is considered, the Bi-LSTM MIMO-NOMA based detector outperforms the SIC MIMO-NOMA detector for the value of $\alpha < 0.07$. The Bi-LSTM MIMO-NOMA detector's performance is shown to be the worst when changes between actual and predicted (channel with estimation error) channel states occurred, although the Bi-LSTM based approach can keep its superiority within a given tolerance.

Table 3. **Modulation techniques used in simulations.**

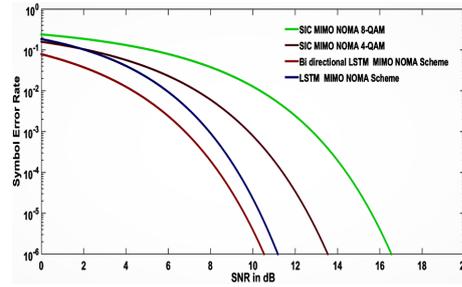| Modulation Scheme	1st UE	2nd UE
1	4-QAM	4-QAM
1	4-QAM	4-QAM
1	4-QAM	4-QAM
1	4-QAM	4-QAM

Fig. 13. SER performance comparison between the Bi-LSTM, LSTM, and SIC-based MIMO-NOMA schemes for 4-QAM and 8-QAM modulation schemes.
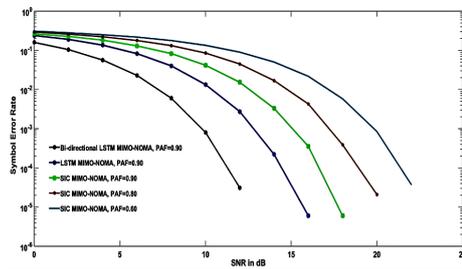

Fig. 14. SER performance comparison for various values of the power allocation factors.
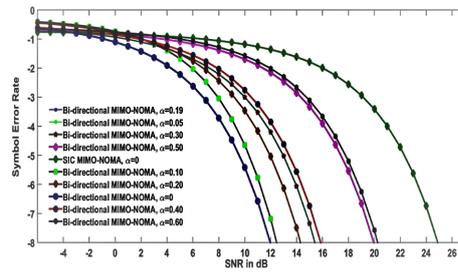

Fig. 15. SER performance comparison between the Bi-LSTM, LSTM, and SIC schemes for various values of channel error factors.

5. CONCLUSION

The perfect and imperfect SIC schemes are explored in this paper, and it is demonstrated that the suggested Bi-LSTM MIMO-NOMA system may increase SER performance over the conventional SIC-based MIMO-NOMA scheme even when the SIC is not perfect. Simulation results with various channel estimation error factors showed the learning performance of the Bi-LSTM MIMO-NOMA. The performance of DL degrades considerably as the channel error factor goes from 0 to 1. Even when the perfect CSI is considered, the DL detector outperforms the SIC NOMA detector for channel error factors smaller than 0.07. The DL detector's performance is shown to be the worst when discrepancies between actual and estimated channel states occurred, whereas the DL-based approach can keep its superiority within a certain tolerance range. Because of its excellent SE and low latency, NOMA is widely acknowledged as having enormous importance in 5G and beyond communication systems. DL has the potential to significantly improve its performance. The unique functions of DL techniques in various NOMA applications are briefly covered in this work. It is explained how DL approaches boost NOMA performance. In addition, the individual DL approaches that have been employed in the literature are given, along with their roles. Finally, a brief discussion on potential future research topics is held.

REFERENCES

1. R. Tiwari and S. Deshmukh, "Handover count based MAP estimation of velocity with prior distribution approximated via NGSIM data-set," *IEEE Transactions on Intelligent Transportation Systems*, Vol. 23, 2021, pp. 4352-4361.

2. T. Ravi and D. Siddharth, "Performance analysis of UABS assisted heterogeneous network for disaster management," in *Proceedings of IEEE 5th International Conference for Convergence in Technology*, 2019, pp. 1-6.

3. L. Chettri and R. Bera, "A comprehensive survey on Internet of Things (IoT) toward 5G wireless systems," *IEEE Internet of Things Journal*, Vol. 7, 2020, pp. 16-32.

4. L. Bhardwaj, R. K. Mishra, and R. Shankar, "Sum rate capacity of non-orthogonal multiple access scheme with optimal power allocation," *The Journal of Defense Modeling and Simulation*, 2021.

5. A. Yadav, C. Quan, P. K. Varshney, and H. V. Poor, "On performance comparison of multi-antenna HD-NOMA, SCMA, and PD-NOMA schemes," *IEEE Wireless Communications Letters*, Vol. 10, 2021, pp. 715-719.

6. S. Ju, Y. Xing, O. Kanhere, and T. S. Rappaport, "Millimeter wave and sub-terahertz spatial statistical channel model for an indoor office building," *IEEE Journal on Selected Areas in Communications*, Vol. 39, 2021, pp. 1561-1575.

7. W. Hong, Z. H. Jiang, C. Yu, D. Hou, H. Wang *et al*., "The role of millimeter-wave technologies in 5G/6G wireless communications," *IEEE Journal of Microwaves*, Vol. 1, 2021, pp. 101-122.

8. A. Zhu, M. Ma, S. Guo, S. Yu, and L. Yi, "Adaptive multi-access algorithm for multi-service edge users in 5G ultra-dense heterogeneous networks," *IEEE Transactions on Vehicular Technology*, Vol. 70, 2021, pp. 2807-2821.

9. G. Gaur, T. Velmurugan, P. Prakasam, and S. Nandakumar, "Application specific thresholding scheme for handover reduction in 5G ultra dense networks," *Telecommunication Systems: Modelling, Analysis, Design and Management*, Vol. 76, 2021, pp. 97-113.

10. R. Shankar, B. K. Sarojini, H. Mehraj, A. S. Kumar, R. Neware, and A. S. Bist, "Impact of the learning rate and batch size on NOMA system using LSTM-based deep neural network," *The Journal of Defense Modeling and Simulation*, 2021.

11. S. Pandya, P. Krishna, R. Shankar, and A. S. Bist, "Examination of the fifth-generation vehicular simultaneous wireless information and power transfer cooperative non-orthogonal multiple access network in military scenarios considering time-varying and imperfect channel state information conditions," *The Journal of Defense Modeling and Simulation*, 2021.

12. M. K. Beuria, R. Shankar, and S. S. Singh, "Analysis of the energy harvesting non-orthogonal multiple access technique for defense applications over Rayleigh fading channel conditions," *The Journal of Defense Modeling and Simulation*, 2021.

13. R. Shankar, T. V. Ramana, P. Singh, S. Gupta, and H. Mehraj, "Examination of the non-orthogonal multiple access system using long short memory based deep neural network," *Journal of Mobile Multimedia*, Vol. 16, 2021, pp. 451-474.

14. M. Aldababsa, M. Toka, S. Gökçeli, G. K. Kurt, and O. Kucur, "A tutorial on nonorthogonal multiple access for 5G and beyond," *Wireless Communications and Mobile Computing*, Vol. 2018, 2018, pp. 9713450.

15. S. Li, L. D. Xu, and S. Zhao, "5G Internet of Things: A survey," *Journal of Industrial Information Integration*, Vol. 10, 2018, pp. 1-9.

16. J. R. Bhat and S. A. Alqahtani, "6G Ecosystem: Current status and future perspective," *IEEE Access*, Vol. 9, 2021, pp. 43134-43167.

17. V. Bhatia, P. Swami, S. Sharma, and R. Mitra, "Non-orthogonal multiple access: An enabler for massive connectivity," *Journal of the Indian Institute of Science*, Vol. 100, 2020, pp. 337-348.

18. V. Andiappan and V. Ponnusamy, "Deep learning enhanced NOMA system: A survey on future scope and challenges," *Wireless Personal Communications*, Vol. 123, 2021, pp. 839-877.

19. Y. Xu, C. Yang, M. Hua, and W. Zhou, "Deep deterministic policy gradient (DDPG)-Based resource allocation scheme for NOMA vehicular communications," *IEEE Access*, Vol. 8, 2020, pp. 18797-18807.

20. G. Gui, H. Huang, Y. Song, and H. Sari, "Deep learning for an effective nonorthogonal multiple access scheme," *IEEE Transactions on Vehicular Technology*, Vol. 67, 2018, pp. 8440-8450.

21. J. Luo, J. Tang, D. K. C. So, G. Chen, K. Cumanan, and J. A. Chambers, "A deep learning-based approach to power minimization in multi-carrier NOMA with SWIPT," *IEEE Access*, Vol. 7, 2019, pp. 17450-17460.

22. C. Lin, Q. Chang, and X. Li, "A deep learning approach for MIMO-NOMA downlink signal detection," *Sensors*, Vol. 19, 2019, No. 2526.

23. D. A. Awan, R. L.G. Cavalcante, M. Yukawa, and S. Stanczak, "Detection for 5G-NOMA: An online adaptive machine learning approach," *arXiv Preprint*, 2017, arXiv:1711.00355.

24. F. Alberge, "Constellation design with deep learning for downlink non-orthogonal multiple access," in *Proceedings of IEEE Annual International Symposium on Personal, Indoor and Mobile Radio Communications*, 2018, pp. 1-5.

25. M. Liu, T. Song, and G. Gui, "Deep cognitive perspective: Resource allocation for NOMAbased heterogeneous IoT with imperfect SIC," *IEEE Internet of Things Journal*, Vol. 6, 2019, pp. 2885-2894.

26. S. Tseng, Y. Chen, C. Tsai, and W. Tsai, "Deep-learning-aided cross-layer resource allocation of OFDMA/NOMA video communication systems," *IEEE Access*, Vol. 7, 2019, pp. 157730-157740.

27. R. Abbas, T. Huang, and B. Shahab, "Grant free non orthogonal multiple access a key enabler for 6G IoT," *arXiv Preprint*, 2020, arXiv.2003.10257.

28. S. Sheikhzadeh, M. Pourghasemian, M. R. Javan, N. Mokari, and E. A. Jorswieck, "AI-based secure NOMA and cognitive radio enabled green communications: Channel state information and battery value uncertainties," *IEEE Dataport*, 2021.

29. Y. Akhmetkaziyev, G. Nauryzbayev, S. Arzykulov, A. M. Eltawil, and K.M. Rabie, "Cognitive non-ideal NOMA satellite-terrestrial networks with channel and hardware imperfections," *IEEE Wireless Communications and Networking Conference*, 2021, pp. 1-6.

30. D. V. Ratnam and K. N. Rao, "Bi-LSTM based deep learning method for 5G signal detection and channel estimation," *AIMS Electronics and Electrical Engineering*, Vol. 5, 2021, pp. 334-341.

31. A. Krishnamoorthy and R. Schober, "Uplink and downlink MIMO-NOMA with simultaneous triangularization," *IEEE Transactions on Wireless Communications*, Vol. 20, 2021, pp. 3381-3396.

32. Y. Saito, Y. Kishiyama, A. Benjebbour, T. Nakamura, A. Li, and K. Higuchi, "Non-orthogonal multiple access (NOMA) for cellular future radio access," in *Proceedings of IEEE 77th Vehicle Technology Conference*, 2014, pp. 1-5.

33. H. Minn and N. Al-Dhahir, "Optimal training signals for MIMO OFDM channel estimation," *IEEE Transactions on Wireless Communications*, Vol. 5, 2006, pp. 1158-1168.

34. L. Liu, C. Liang, J. Ma, and L. Ping, "Capacity optimality of AMP in coded systems," *arXiv Preprint*, 2020, arXiv:1901.09559v3.

35. A. Ly and Y.-D. Yao, "A review of deep learning in 5G research: Channel coding, massive MIMO, multiple access, resource allocation, and network security," *IEEE Open Journal of the Communications Society*, Vol. 2, 2021, pp. 396-408.

36. M. A. Alsheikh, D. Niyato. S. Lin, H.-P. Tan, and Z. Han, "Mobile big data analytics using deep learning and apache spark," *IEEE Network*, Vol. 30, 2016, pp. 22-29.

37. M. AbdelMoniem, S. M. Gasser, M. S. El-Mahallawy, M. W. Fakhr, and A. Soliman, "Enhanced NOMA system using adaptive coding and modulation based on LSTM neural network channel estimation," *Applied Sciences*, Vol. 9, 2019, No. 3022.

38. P. Bento, J. Pombo, S. Mariano, and M. d. R. Calado , "Short-term load forecasting using optimized LSTM networks via improved bat algorithm," in *Proceedings of International Conference on Intelligent Systems*, 2018, pp. 351-357.

Ravi Shankar received his Ph.D. in Wireless Communication from the NIT Patna, Patna, India, in 2019. His current research interests cover cooperative communication, D2D communication, IoT/M2M networks and network protocols.

Manoj Kumar Beuria is pursuing PhD from KIIT University, India. His current research interests include wireless communication, information propagation analysis, NOMA, deep learning machine learning.

Gopal Ramchandra Kulkarni is working as a Principal at Merchant Engineering College, Basna, India. His current research interests include Social Network Analysis, Information Propagation Analysis, web-based network analysis, Machine Learning.

Abu Sarwar Zamani is working as a Professor at Prince Sattam bin Abdulaziz University, Alkharj Saudi Arabia. His current research interests include Social Network Analysis, Information Propagation Analysis, web-based network analysis, Machine Learning.

Patteti Krishna is working as a faculty at Netaji Subhas University of Technology East Campus, New Delhi, India.He has obtained Doctoral (Ph.D) Degree in Electronic and Communication Engineering (ECE), from Jawaharlal Nehru Technological University, Hyderabad in 2017.

V Gokula Krishnan is working as an Assistant Professor at Department of Computer Science and Information Technology, CVR College of Engineering, India. His current research interests include Deep neural network, cooperative wireless communication, web-based network analysis, Machine Learning.